

COVER SHEET

*NOTE: This coversheet is intended for you to list your article title and author(s) name only
—this page will not appear on the CD-ROM.*

Title and author(s) will be inserted by the publisher on the first page, above the abstract.

Title: *Numerical modeling of heat transfer in steel-concrete composite slabs*

Authors: Jian Jiang,
Joseph A. Main,
Jonathan M. Weigand,
Fahim Sadek

ABSTRACT

This paper presents detailed and reduced-order numerical modeling of heat transfer in composite floor slabs with profiled steel decking for analysis and design of structures exposed to fire. The detailed modeling approach represents the concrete slab with solid elements and the steel decking with shell elements. The reduced-order modeling approach represents the thick and thin parts of a composite slab with alternating strips of layered shell elements. The detailed modeling approach was validated against experimental results available in the literature, and the reduced-order modeling approach was calibrated and verified against the detailed model results. A parametric study using the detailed modeling approach was conducted to investigate the influence of slab geometry on the temperature distribution within composite slabs. The results show that the rib height of the decking and the width at the top of the rib are key factors governing the temperature distribution in the rib. The paper also presents comparisons with Eurocode 4 calculations of fire resistance of composite slabs. The comparisons indicate that the Eurocode 4 overestimates the fire resistance compared to the numerical results by up to 12 %.

INTRODUCTION

Typical steel/concrete composite floor slab construction consists of a concrete topping on profiled steel decking, typically reinforced with welded wire mesh. The decking acts as reinforcement and permanent formwork, reducing materials and construction time. One of the advantages of this type of construction when exposed to fire is the shielding effect provided by the ribs, which limits the temperature rise in the reinforcement. However, the presence of the ribs creates an orthotropic profile, which results in thermal and structural responses that are more complex than those for flat slabs, presenting challenges in numerical analysis and practical design.

The objective of this study is to develop a reduced-order modeling approach for heat transfer analysis of composite slabs that is also suitable for structural analysis, so that the same model can be used for thermal and structural analysis. Previous heat transfer analyses have generally used a detailed finite-element modeling approach, with solid elements for the concrete slab and shell elements for the steel decking [1-3]. In considering the suitability for heat transfer analysis of reduced-order modeling approaches previously used for structural analysis, the grillage approach with beam elements [4] has significant limitations, because of the inadequacy of the 1D elements to represent in-plane and through-thickness heat transfer in the slab. Modeling approaches that use a constant shell thickness [5] also have limitations for thermal analysis because they fail to capture the shielding effect of the ribs, which results in curved isotherms in the floor slab, significantly affecting both the structural response and the thermal insulation provided by the slab. The modeling approach that uses alternating strips of shell elements in structural analyses [6], however, has the potential to capture both in-plane and through-thickness heat transfer in composite slabs.

In this study, a detailed finite-element model was first developed and validated for heat transfer analysis in composite floor slabs. This approach was then used to conduct

a parametric study by varying the geometric parameters of the slab to examine their influence on the slab's thermal response. The numerical results were compared against calculations based on Eurocode 4 (EC4) [7]. A reduced-order modeling approach consisting of layered shell elements was then proposed and verified against the detailed model.

DETAILED NUMERICAL MODELING

The heat transfer analysis of composite slabs was performed using the finite element software LS-DYNA¹ [8]. Noting the periodicity of the composite slab profile, only one half-strip of the composite slab was modeled, with adiabatic boundary conditions at the right and left boundaries, as shown in Figure 1. The concrete slab was modeled with solid elements and the steel decking was modeled with shell elements. The concrete slab and steel decking had a consistent mesh at their interface and shared common nodes. The model used temperature-dependent thermal properties of concrete and steel based on EC4 [7].

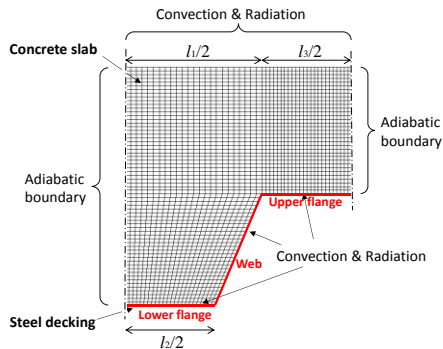


Figure 1. Schematic of the detailed model

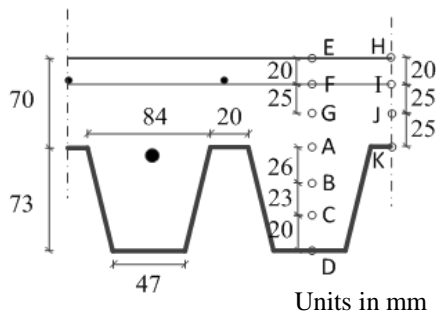


Figure 2. Geometry of the tested slab [1].

The detailed modeling approach was validated against a standard fire test denoted as Test 2 in [1]. The tested slab had 6 ribs and used Prins PSV73¹ steel decking and normal weight concrete with a measured moisture content of 3.4 %. The effect of moisture content is accounted for in the temperature-dependent specific heat model from EC4. The geometry of the tested slab is shown in Figure 2. Thermal boundary conditions at the top and bottom of the slab were taken from [1], and gas temperatures applied to the bottom surfaces were based on ISO 834 [9]. Numerical and experimental results for several points shown in Figure 2 are compared in Figure 3. The difference between the measured and computed temperatures did not exceed 15 % (Point B at time 80 minutes).

¹ Certain commercial entities, equipment, products, or materials are identified in this document in order to describe a procedure or concept adequately. Such identification is not intended to imply recommendation, endorsement, or implication that the entities, products, materials, or equipment are necessarily the best available for the purpose.

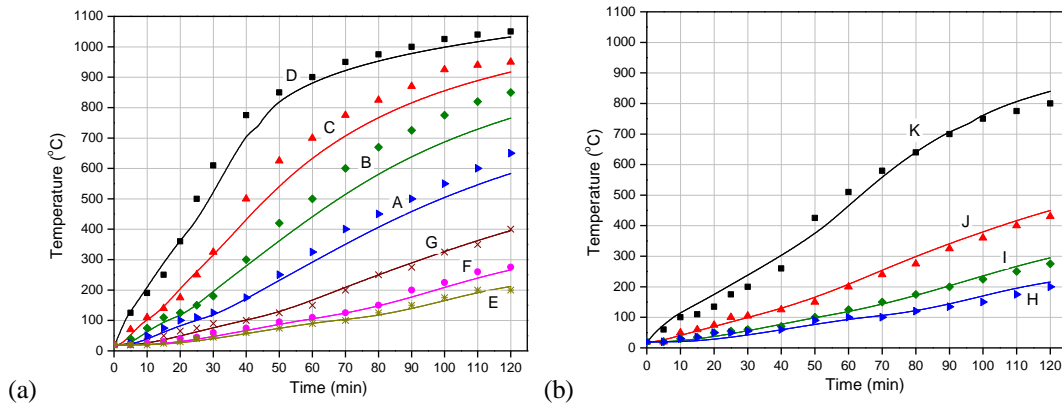


Figure 3. Comparison of calculated (solid curves) and measured² (discrete symbols) temperatures: (a) in the thick part; (b) in the thin part.

PARAMETRIC STUDY

The detailed modeling approach was used to perform a parametric study on the thermal behavior of composite slabs. Vulcraft 3VLI¹ decking, commonly used in North America, was selected as the baseline configuration for the parametric study. The selected geometry is depicted in Figure 4. The thickness of the steel decking was 0.9 mm and lightweight concrete was used. The same modeling approach and thermal loading as in the previous section was used in the parametric study. Figure 5 shows the predicted temperature distribution in the slab for the baseline configuration after three hours. Inclined temperature contours indicate non-uniform heat transfer through the composite slab, resulting from the profiled shape of the steel decking.

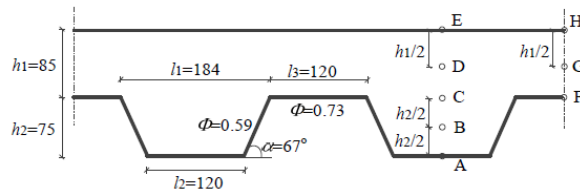


Figure 4. Configuration of the slab Vulcraft 3VLI (all dimensions are in mm).

Considering the practical ranges of geometric parameters (h_1 , h_2 , l_1 , l_2 , and l_3), the parametric study used values of $h_1 = (50 \text{ mm}, 85 \text{ mm}, 125 \text{ mm})$, $h_2 = (50 \text{ mm}, 75 \text{ mm}, 100 \text{ mm})$, $l_1 = (130 \text{ mm}, 184 \text{ mm}, 250 \text{ mm})$, $l_2 = (80 \text{ mm}, 120 \text{ mm}, 160 \text{ mm})$, and $l_3 = (80 \text{ mm}, 120 \text{ mm}, 160 \text{ mm})$. Only one geometric parameter was changed at a time, with all other parameters having the values shown in Figure 4. The results are shown in Figure 6. The parameter h_1 had a significant influence on the temperature of the unexposed surface of the slab (Point E) as shown in Figure 6a. The height of the rib, h_2 , and the width at the top of the rib, l_1 , affected the temperature in the rib (Point C) more

² The policy of the National Institute of Standards and Technology is to include statements of uncertainty with all NIST measurements. In this document, however, measurements of authors outside of NIST are presented, for which uncertainties are not reported and are unknown.

significantly than they affected the temperature at the unexposed surface (Point E), as shown in Figures 6b and 6c. The temperature in the slab increased as h_2 and l_1 decreased, due to the reduced amount of concrete in the rib. Compared to h_2 and l_1 , the dimensions l_2 and l_3 had a less significant effect on the temperature at point C (Figures 6d and 6e). However, the width of the upper flange of the deck, l_3 , along with the height of the concrete topping, h_1 , governed the heat transfer through the thin part of the slab, where the maximum temperature at the unexposed side occurred (Point H).

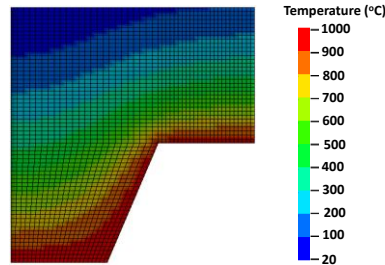


Figure 5. Temperature contours in the baseline slab configuration after three hours.

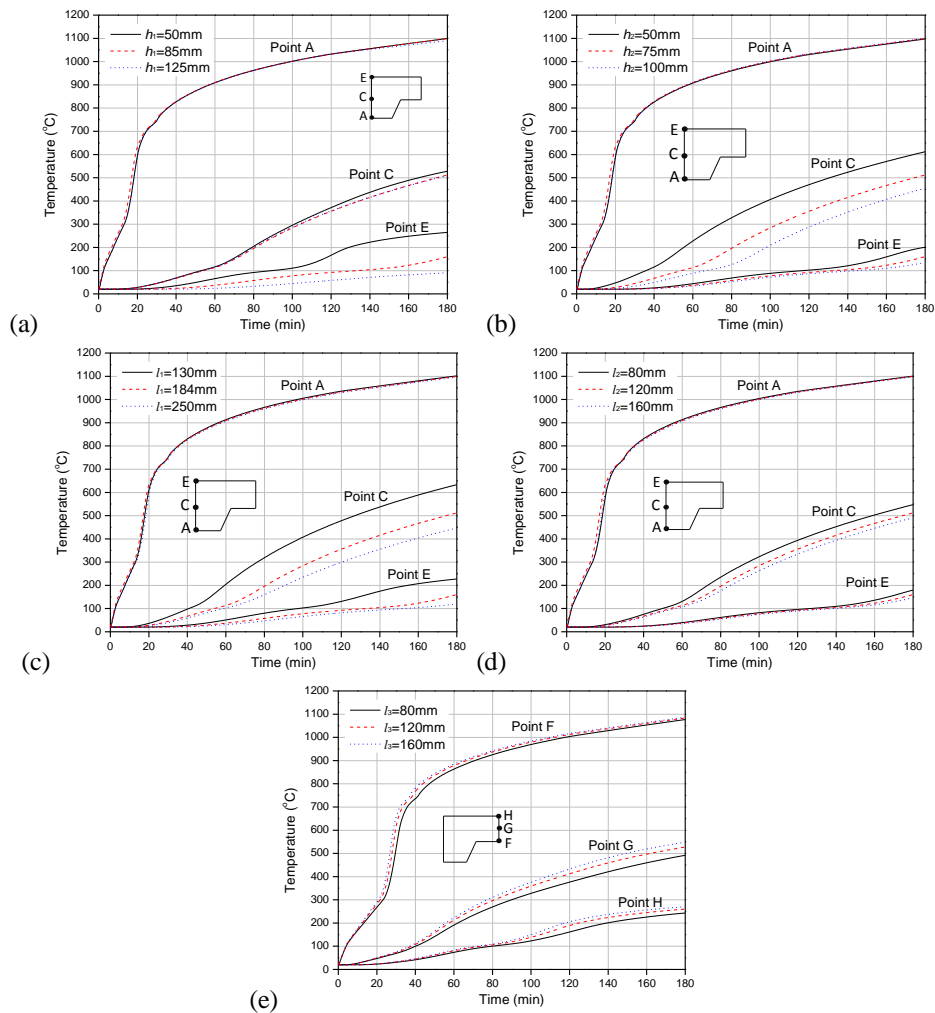


Figure 6. Variation of temperature within the slab against: (a) h_1 ; (b) h_2 ; (c) l_1 ; (d) l_2 ; (e) l_3 .

Table 1 presents a comparison of fire resistances for composite slabs estimated from Annex D in EC4 calculations [7] and from numerical analyses. The fire resistance in EC4, expressed in minutes, is based on the fire duration until a maximum temperature of 180 °C or an average temperature of 140 °C, whichever governs, is achieved at the unexposed surface of the slab. As shown in Table 1, the fire resistance of the composite slabs, based on the numerical results, was governed by the maximum temperature (Max) occurring at the unexposed surface of the slab, rather than by the average temperature (Ave). The table indicates that the EC4 calculation overestimates the fire resistance compared with the numerical results by up to 12.3 %. The overestimation of fire resistance would be even greater in comparison with the experimental data because, as shown Fig. 3, the numerical results underestimate the temperatures by as much as 15 %. This overestimation of fire resistance in the EC4 calculation may be is likely due to an underestimation of the effect of the upper flange width, l_3 , which was a key factor influencing the maximum temperature at the top surface of the thin part of the slab.

TABLE 1. COMPARISON OF FIRE RESISTANCE BETWEEN EC4 CALCULATIONS AND NUMERICAL PREDICTIONS

Varied parameters	Fire resistance (min)					
	EC4 Annex D	Detailed Numerical				
		Max	Difference (%)	Ave	Difference (%)	
h_1	50 mm	64	55	14	60	6.25
	85mm	140	124	11.4	136	2.9
	125 mm	227	247	8.8	249	9.7
h_2	50 mm	131	121	7.6	124	5.3
	75 mm	140	124	11.4	136	2.9
	100 mm	146	128	12.3	136	6.8
l_1	130 mm	135	128	5.2	130	3.7
	184 mm*	N/A	124	–	136	–
	250 mm*	N/A	121	–	130	–
l_2	80 mm	137	122	10.9	127	7.3
	120 mm	140	124	11.4	136	2.9
	160 mm*	N/A	128	–	135	–
l_3	80 mm	147	139	5.4	143	2.7
	120 mm	140	124	11.4	136	2.9
	160 mm*	N/A	117	–	123	–

*Asterisk indicates parameters are beyond range of EC4 calculation method.

REDUCED-ORDER NUMERICAL MODELING

The reduced-order modeling approach was developed using a layered composite shell formulation, in which a distinct structural material, thermal material, and thickness can be specified for each layer, including layers to represent fireproofing, if needed. The proposed approach uses alternating strips of shell elements to represent the thick and thin parts of composite slabs, as illustrated in Figure 7. For the half-strip configuration in Figure 1, only two shell elements were used, with the width of the thick and thin parts each being spanned by a single shell element. The tapered profile of the slab rib was accounted for in Shell A by reducing the density of concrete in the rib to ensure accurate representation of the mass of concrete in each layer (i.e., ρ_1, ρ_2, \dots in Figure 7), since the

shell formulation assumes constant width of all layers. The reduced concrete density in the i^{th} layer of the rib, ρ_i , was calculated based on the ratio of the average rib width for that layer, d_i , to the total width at the top of the rib, l_1 (i.e., $\rho_i = \rho_0 \times d_i / l_1$).

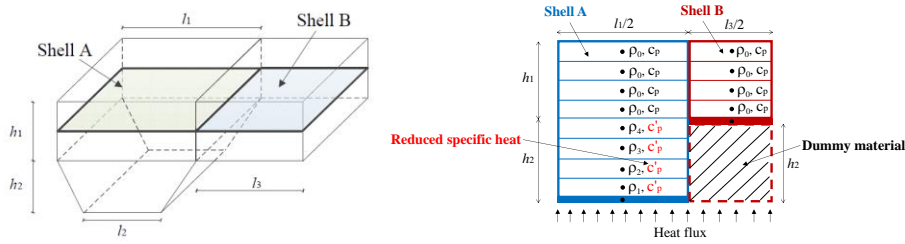


Figure 7. Schematics illustrating reduced-order modeling of composite slabs.

In modeling the thin part of the slab (Shell B), a “dummy material” with high thermal conductivity and negligible specific heat was used to represent the absence of material below the steel decking. The use of the dummy material allowed Shell A and Shell B to be modeled with the same thickness, so that in-plane heat conduction between corresponding layers of adjoining shell elements could be properly accounted for. Thermal boundary conditions were applied at the fictitious bottom surface of Shell A, and the high thermal conductivity of the dummy material ensured an essentially equivalent temperature at the top of the dummy material, thus providing appropriate thermal boundary conditions for the steel decking. The essentially uniform temperature through the depth of the dummy material also provided thermal loading to the adjoining layers in the rib of Shell A, thus partially accounting for heat input through the web of the decking. Analysis of the reduced-order model was carried out with the same material characterization and thermal loading as the detailed model in the previous section. Figure 8 shows a comparison of the calculated temperature histories from the detailed and reduced-order models for the composite slab. The largest difference between the results of the two models is at point M, where the temperatures differed by about 16 % at the end of the analyses. This difference was found to be much larger when the dummy material was not used, and the remaining difference (16 %) resulted from not completely accounting for the heat input through the web of the decking within the layered shell formulation.

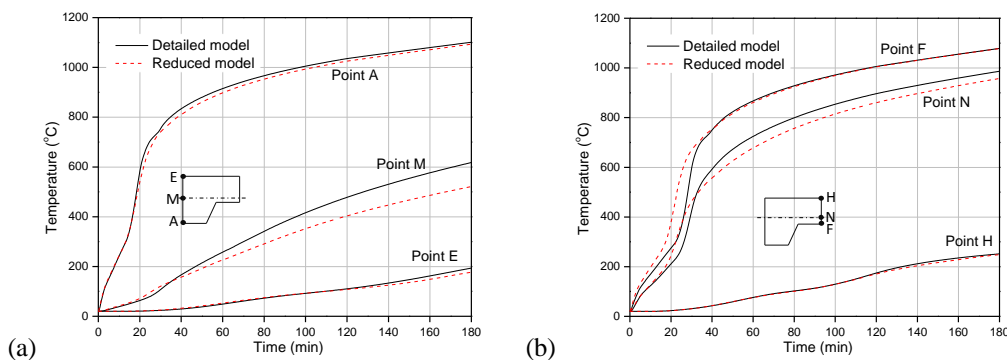


Figure 8. Comparison of average temperature histories for detailed and reduced models: (a) in the thick part; (b) in the thin part.

To improve the accuracy of the reduced-order model, the specific heat of concrete in the rib, c'_p (see Figure 7), was reduced to compensate for the delayed heating observed above the rib in Shell A (point M in Figure 8). The optimum value of c'_p was determined by minimizing the differences in the calculated temperatures at point M between the detailed and reduced-order models. Figure 9 shows the overall difference in temperature, T_{gap} , between the detailed model and the reduced-order models with different values of c'_p , calculated as follows:

$$T_{gap} = \sqrt{\frac{\sum_{i=1}^n (T_{reduced} - T_{detailed})^2}{n}}, \quad (1)$$

where n is the number of time samples. The minimum value of $T_{gap} = 14^\circ\text{C}$ corresponded to $c'_p = 0.7c_p$, and Figure 10 shows the resulting temperature distribution for this optimum value. The computed temperatures from the detailed and reduced-order models differed by 5 % or less. The influence of the slab geometry on the optimal value of c'_p has been investigated and will be presented in a future publication.

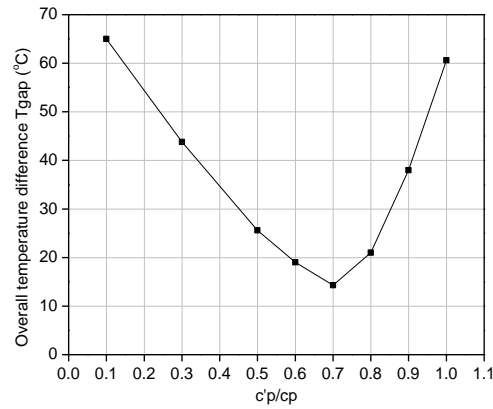


Figure 9. Overall temperature difference at the middle surface of Shell A (Point M) against various values of reduced specific heat.

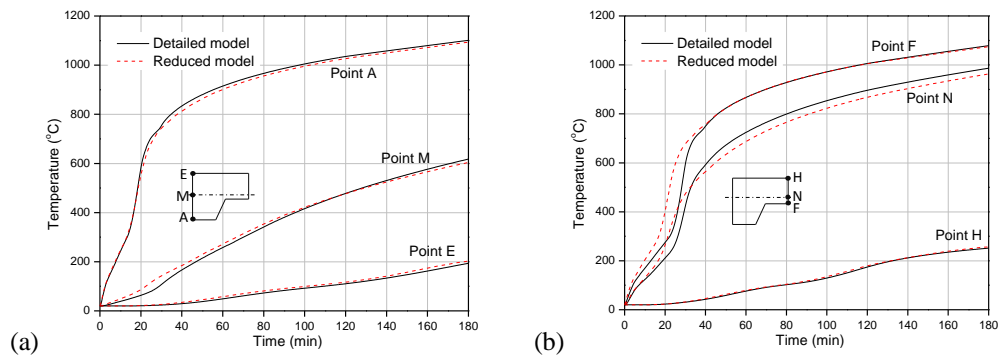


Figure 10. Comparison of temperature histories for detailed and reduced models with reduced specific heat of $c'_p=0.7c_p$: (a) in the thick part; (b) in the thin part

SUMMARY AND CONCLUSIONS

This paper presented detailed and reduced-order finite element models for heat transfer in composite floor slabs with profiled steel decking. The detailed modeling approach represented the concrete slab with solid elements and the steel decking with shell elements. The reduced-order modeling approach represented the thick and thin parts of a composite slab with alternating strips of layered shell elements. The detailed modeling approach was validated against experimental results available in the literature, and the reduced-order modeling approach was verified and calibrated against the detailed model results. A parametric study using the detailed modeling approach was conducted to investigate the influence of slab geometry on the temperature distribution within composite slabs. The results showed that the rib height of the steel decking and the width at the top of the rib are key factors affecting the temperature distribution in the rib. The heat input through the web of the steel decking also plays a key role in the non-uniform temperature distributions in the horizontal plane of slabs. It is possible to account for this web heat input in reduced-order models (shell elements) by reducing the specific heat of concrete in the rib and adding dummy material with low specific heat and high thermal conductivity in the thin part of the slab. The paper also presented comparisons with Eurocode 4 calculations of fire resistance of composite slabs. The results showed that the fire resistance of composite slabs, based on the thermal insulation criterion, was governed by the maximum temperature at the unexposed surface, rather than the average temperature. The comparison indicated that the Eurocode 4 overestimates the fire resistance compared to the numerical results by up to 12 %.

REFERENCES

1. Hamerlinck R., Twilt L. and Stark J. 1990. "A Numerical Model for Fire-exposed Composite Steel/concrete Slabs," presented at the 10th International Specialty Conference on Cold-formed Steel Structures, USA, 1996.
2. Guo S. 2012. "Experimental and Numerical Study on Restrained Composite Slab during Heating and Cooling," *Journal of Constructional Steel Research*, 69: 95-105.
3. Pantousa D. and Mistakidis E. 2013. "Advanced Modelling of Composite Slabs with Thin-walled Steel Sheeting submitted to Fire," *Fire Technology*, 49: 293-327.
4. Elghazouli A. Y., Izzuddin B. A., and Richardson A. J. 2000. "Numerical Modelling of the Structural Fire Behaviour of Composite Buildings," *Fire Safety Journal*, 35: 279-297.
5. Huang Z., Burgess I. W. and Plank R. J. 2000. "Effective Stiffness Modelling of Composite Concrete Slabs in Fire," *Engineering Structures*, 22(9): 1133-1144.
6. Main J.A. and Sadek F. 2012. "Robustness of Steel Gravity Frame Systems with Single-Plate Shear Connections," *NIST TN-1749*, National Institute of Standards and Technology, Gaithersburg, MD.
7. European Committee for Standardization (CEN). 2005. Eurocode 4 Design of composite steel and concrete structures: Part 1.2: General rules, Structural fire design, EN 1994-1-2, Brussels.
8. Livermore Software Technology Corporation (LSTC). (2012), LS-DYNA Keyword User's Manual, Version 971, Livermore, CA.
9. International Organization for Standardization (ISO). 2014. *Fire-resistance tests – Elements of building construction, ISO 834-11*, Geneva, Switzerland.